Vol. 39, No. 4 (2017) 431-443, DOI: 10.24874/ti.2017.39.04.02

Tribology in Industry

www.tribology.fink.rs

RESEARCH

Effect of Changing Ellipiticity Ratio on the Formation of Ultra-Thin Lubricating Film

M.F. Abd Al-Samieh[a]

[a]*Mechanical design and production Department, Military Technical College, Cairo, Egypt.*

Keywords:

Ultra-thin films
Elastohydrodynamics
Solvation
Van der Waals' force
Ellipiticity ratio

Corresponding author:

M.F. Abd Al-Samieh
Mechanical design and production Department, Military Technical College, Cairo, Egypt.
E-mail: mohamed.fahmy203@hotmail.com

A B S T R A C T

The mechanism of fluid film lubrication in ultra-thin conjunction under elliptical point contacts is discussed in this paper. The results of changing the ellipticity ratio are highlighted. The operating conditions; load and speed of entraining motion, promote formation of ultra-thin films that are formed under the combined action of Elastohydrodynamic lubrication (EHL), surface contact force of solvation and molecular interactions due to presence of Van der Waals' force. The paper shows that, changing the ellipticity ratio maintain the general behavior of the formation of ultra-thin lubricating film thickness as in the case of circular point contact problem when the contiguous solids are subject to light-to-medium contact loads and the effects of surface forces become significant as the elastic film (i.e. the gap) is reduced to a few nanometers and lubricant discretisation appears.

1. INTRODUCTION

In recent years there has been a growing trend toward component miniaturisation in the manufacture of increasingly compact and lightweight machines. This has opened new fields of engineering endeavour such as micro-engineering and nano-technology, with diverse applications. As a sequence of this, the separation of load surfaces has reduced considerably under the operating conditions; such as load and relative motion of contiguous bodies. Under these conditions the lubricant behaviour is no longer governed purely by its bulk properties such as density and viscosity as shown by Becker and Mugele [1], Tanner and Jabbarzadeh [2] and Manojlović [3]. They found that a confined liquid films with a thickness in the range of a few molecular diameters exhibit different mechanical properties than in the bulk and the viscosity increased by a factor of 10 with decreasing the film thickness from 6 to 2 layers enables an increased load capacity to be sustained in such films. Such films are formed in micro-devices such as micro-gears used mainly in sensitive monitoring equipment, where their low inertia makes them insensitive to vibration. A good application is in MEMS (Micro-Electro-Mechanical Systems) applications as shown by Xiankun Cao et al. [4], microelectromechanical gears and actuators [5], immersed particles or soft jells colliding with smooth barriers as shown by Xiaobai et al. [6].

In 1985 Chan and Horn [7] pointed out that for molecularly smooth surfaces, the Reynolds equation seems to apply down to a film thickness of 50 nm, and even further down to several nanometres simple correction factors can be applied. At closer distances, attractive Van der Waals' force and the oscillatory (attraction-repulsion) solvation force become the dominant mechanisms in lubricant film formation. Jang and Tichy [8] have presented a full numerical solution for the problem of EHL, including the effect of the Van der Waals' force and solvation pressure. However, their investigation shows little effect from the surface and molecular forces, even down to a film thickness of 2 nm. Jianbin Luo et al. [9] showed experimentally using relative optical interference intensity technique that the hydrodynamic effect can be clearly observed even at very low speed if the contact pressure is sufficiently low or if the viscosity of lubricant is comparatively high. When the pressure increases to a certain degree, the film thickness will suddenly drop to the dimension of several layers of molecules and this is where the failure of the fluid film has taken place. Hartl et al. [10] measure the very thin lubrication films down to one nanometer in a point contact between a steel ball and a transparent disc using colorimetric interferometry. They found that both hexadecane and mineral base oil obey the linear relationship between log central and minimum film thickness and log rolling speed predicted by elastohydrodynamic theory down to approximately one nanometer. Morales-espejel et al. [11] found that new controversy concerning the film thickness-velocity dependence in EHL contacts at very low speeds and high loads, with some predictions showing a film thickness much less than that predicted by the classical equations. It has been also reported in the past through experimental studies that a lubricant film thickness more than 50 nm by Dalmaz [12], 15 nm by Johnston et al. [13] and 10 nm by Cooper and Moore [14] agrees well with the theoretical prediction of Hamrock and Dowson [15] film thickness formula. Glovnea et al. [16] found expeperimentally that no evidence of film thickness collapses at low speeds even at high pressure. Instead, the observed behavior has been found to conform closely to the Hamrock-Dowson classical regression equation. A number of researchers [17,18] have shown that with certain lubricants, the effect of surface forces is negligible and that the lubricant film behaviour follows the EHL theory down to the thickness of 1 nm The physical explanation for this put forward by Christensen et al. [19] and Gee et al. [20] was that these lubricants have either a chain or branched structure, and owing to their flexibility entangle and exhibit little solvation effect adjacent to the solid surface.

Matsouka and Kato [21] and Al-samieh and Rahnejat [22] have presented a full numerical solution for the problem of EHL, including the effect of the Van der Waals' force and solvation pressure under circular point contact. They found that when the film thickness is more than 10 nm there is a good agreement with the conventional continuum fluid lubrication theory, and in the case of film thickness values, less than 10 nm, discretization of the film was observed. These findings corroborated the experimental predictions reported by Kato and Matsouka [23]. Recently, Al-samieh [24] has extended the work reported in reference [22] to develop a numerical solution for the problem of EHL, including the effect of the Van der Waals' force and solvation pressure under elliptical point contact. The results were restricted to the case of elliptical ratio of 6 and showed that when the film thickness is more than 7 nm there is a good agreement with the conventional continuum fluid lubrication theory, and in the case of film thickness values, less than 7 nm, discretization of the film was observed as that found in circular point contact problem.

In this paper a large range of loads (0.01-10) mN, ellipiticity ratio of (2-6) and speed of 0.2 mm/s are employed to investigate the effect of changing the ellipiticity ratio on the formation of ultra-thin lubricating films under isothermal conditions. The solution method includes the effect of solvation pressure, as well as the Van der Waals' force with regard to ultra-thin conjunctions.

2. BACKGROUND THEORY

In the conventional EHL theory, film thickness and pressure distribution are obtained by simultaneous solution of the Reynolds' equation, the elastic film shape, incorporating the contact deformation of the semi-infinite solid (given by the elasticity equation) and the load balance equation. However, in the case of ultra-thin film

thickness a pressure caused by the Van der Waals' inter-molecular forces and solvation pressure due to inter-surface forces should be considered. The total pressure P, is composed of three components, solvation pressure; P_s, Van der Waals' pressure contribution; P_{vdw}, and conventional viscous pressure; P_h:

$$P = P_s + P_{vdw} + P_h \quad (1)$$

This approach was established by Matsuoka and Kato [21] and Al-Samieh and Rahnejat [22].

2.1 Elastohydrodynamic Pressure

The dimensionless Reynolds' equation for elliptical point contact condition in a general form can be written as:

$$\frac{\partial}{\partial X}\left(\frac{\bar{\rho}H^3}{\bar{\eta}}\frac{\partial P_h}{\partial X}\right)+\frac{\partial}{\partial Y}\left(\frac{\bar{\rho}H^3}{\bar{\eta}}\frac{\partial P_h}{\partial Y}\right)=\lambda\left\{\frac{\partial(\bar{\rho}H)}{\partial X}+\frac{bE'}{\eta_o u}\left(\bar{\rho}\frac{\partial H}{\partial \bar{t}}+H\frac{\partial \bar{\rho}}{\partial \bar{t}}\right)\right\} \quad (2)$$

Under steady-state entraining motion, the squeeze film term is neglected and the above equation (2) can be reduced to:

$$\frac{\partial}{\partial X}\left(\frac{\bar{\rho}H^3}{\bar{\eta}}\frac{\partial P_h}{\partial X}\right)+\frac{1}{K^2}\frac{\partial}{\partial Y}\left(\frac{\bar{\rho}H^3}{\bar{\eta}}\frac{\partial P_h}{\partial Y}\right)=\lambda\frac{\partial}{\partial X}(\bar{\rho}H) \quad (3)$$

Where the following dimensionless variables apply:

$X=x/b$, $Y=y/a$, $\bar{\eta}=\eta/\eta_0$, $\bar{\rho}=\rho/\rho_0$, $H=hR_x/b^2$, $P_h=p_h/p_{Her.}$

and: $\lambda=\dfrac{12u\eta_o R_x^2}{b^3 P_{Her}}$

The variation in density of the lubricant with pressure is defined by Dowson and Higginson [25] as:

$$\bar{\rho}=1+\frac{\varepsilon P_h P_{Her}}{1+\xi P_h P_{Her}} \quad (4)$$

where ε and ζ are constants, dependent upon the type of lubricant used and their values for OMCTS are shown in Table 1 below. The variation in the viscosity of the lubricant with pressure in dimensionless form is given by Roelands [26] as:

$$\bar{\eta}=\exp\left[\ln\eta_\circ+9.67\right]\left[\left(1+5.1*10^{-9}P_h P_{Her}\right)^Z-1\right] \quad (5)$$

where: $Z=\dfrac{\alpha}{5.1*10^{-9}\left[\ln\eta_\circ+9.67\right]}$

where η_0 is the atmospheric lubricant viscosity and α is the pressure of viscosity coefficient. Their values for Octamethylcyclotetrasiloxane (OMCTS) equal 2.35 mPa.s, and 10 GPa^{-1} respectively.

The elastic film shape in dimensionless form is assumed to be of the same as that reported by Hamrock and Dowson [27], given by:

$$H(X,Y)=H_\circ+\frac{(X-m)^2}{2}+\frac{K^2R_x}{R_y}\frac{(Y-l)^2}{2}+\frac{R_x\delta(X,Y)}{b^2} \quad (6)$$

where, the dimensional elastic deformation at any point x, y is defined by Hamrock and Dowson [27] as:

$$\delta_{I,J}(x,y)=\frac{2}{\Pi}\sum_{j=1}^{ny}\sum_{i=1}^{nx}P_{i,j}D_{i^*,j^*} \quad (7)$$

where: $i^*=|I-i|+1,\ j^*=|J-j|+1$

The Newton-Raphson method is applied for the solution of the Reynolds'equation in the following numerical form:

$$\sum_{l=2}^{my-1}\sum_{k=2}^{mx-1}J_{k,l}^{i,j}\Delta\bar{P}_{k,l}=-F_{i,j} \quad (8)$$

Where, the Jacobian matrix is a tensorial quantity, given in terms of the residual derivatives as:

$$J_{k,l}^{i,j}=\frac{\partial F_{i.j}}{\partial P_{k,l}} \quad (9)$$

Using the Gauss-Seidel iteration method, the system state equation can be written as:

$$\Delta P_{k,l}^n=(-F_{i,j}-J_{k-1,l}^{i,j}\Delta P_{k-1,l}^n-J_{k+1,l}^{i,j}\Delta P_{k+1,l}^{n-1}-J_{k,l-1}^{i,j}\Delta P_{k,l-1}^n-J_{k,l+1}^{i,j}\Delta P_{k,l+1}^{n-1})/J_{k,l}^{i,j} \quad (10)$$

Where n is the iteration counter in the above recursive equation.

For the reason of good numerical stability an under-relaxation factor is employed to update the pressure according to:

$$P_{i,j}^n=P_{i.j}^{n-1}+\Omega\Delta P_{i,j}^n \quad (11)$$

where Ω is the under-relaxation factor, typically chosen as 0.01 under the reported conditions in this paper.

The convergence criterion on the pressure is:

$$\left[\frac{\sum_i\sum_j\left(\bar{P}_{i,j}^n-\bar{P}_{i,j}^{n-1}\right)^2}{N}\right]^{0.5}\le 10^{-4}$$

The convergence criterion on load balance is given as:

$$\left| \int\int P(X,Y)dXdY - \frac{2}{3}\pi \right| \le 10^{-4}$$

The ellipticity parameter is a function of the radii of curvature of the solids (r_{Ax}, r_{Bx}, r_{Ay}, and r_{By}). The radii of curvature in the x-direction for both solids A and B are used in defining in the dimensionless speed and load parameters. Therefore, only the radius of solid B in the y-direction was changed in varying the ellipticity parameter (K). Figure 1 shows two contacting solids A and B can be made equivalent to that between a single ellipsoidal solid near a plane.

The boundary conditions are the following:

$$P_{hi,1} = P_{hi,N} = P_{h1,j} = P_{hM,j} = 0$$

$$P_h = \frac{\partial P_h}{\partial X} = \frac{\partial P_h}{\partial Y} = 0$$

Note that the boundary conditions are applied to the case of the mechanism that promotes formation of a continuum, in this case the hydrodynamic viscous action

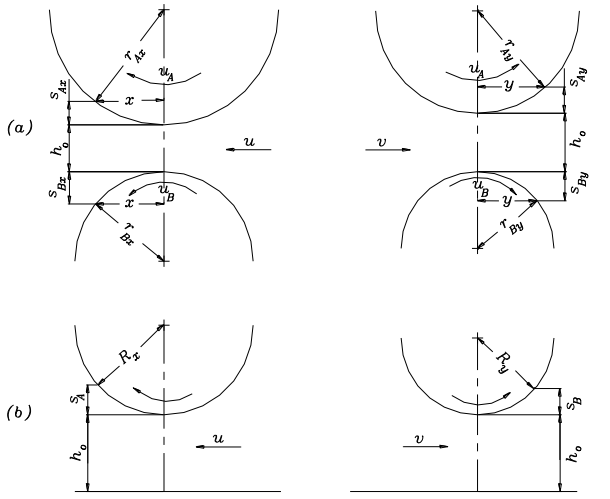

Fig. 1. Geometry of equivalent ellipsoidal solids near a plane; a) Two different ellipsoidal rigid solids in x=0 and y=0 planes; b) Equivalent ellipsoidal solid near a plane in x=0 and y=0 planes.

2.2 Solvation Pressure

Solvation force (i.e. structural force) is a surface interaction force that acts between two solid surfaces, when they approach each other to form a very small gap filled by a fluid. Van Megen and Snook [28], Horn and Israelachvili [29], Israelachvili et al. [30], Homola et al. [31], Israelachvili [32], Philippe Bordarier et al. [33] and Ateeque Malani and Ayappa [34] have studied the solvation force in the narrow contact of contiguous bodies. They have all shown that these surface forces have generally a decaying oscillatory characteristic as a function of gap (i.e. the film thickness). They vary as attractive and repulsive forces, with a periodicity equal to the mean diameter of the fluid molecules. Such oscillatory forces arise from the molecular geometry and local structure of the liquid medium, and reflect the forced ordering of the liquid molecules into discrete layers, when constrained between two surfaces.

In 1985 Chan and Horn [7] performed experiments to measure the thickness of liquid films as a function of time as they are squeezed between two molecularly smooth Mica surfaces. They incorporated the hydrodynamic and the surface force effects. From their experimental work, they proposed the following exponential-cosine model for the solvation force,

$$P_s = -Ce^{\frac{-h}{a}} \cos(2\pi h/a) \qquad (12)$$

where for OMCTS: a=1 nm, C=172 MPa.

Therefore, equation (12) is an empirical relationship for generated solvation pressures derived from experimental observation. The exact solution of the solvation pressure is obtained analytically using model based on the work of Ornstein-Zernike integral equation [35].

2.3 Van der Waals' Pressure

Van der Waals' forces of attraction exist between two surfaces, when they are separated by a very thin fluid film (see for example, lifshitz [36]). Israelachvili [32] gives the pressure in the fluid, induced by the Van der Waals' forces as a function of separation as:

$$P_{vdw} = \frac{-A}{6\pi h^3} \qquad (13)$$

For OMCTS: $A=10^{-20}$ Joules.

The total pressure in "equation (1)" is calculated simultaneously with the elastic film shape "equation (6)" in the same manner as that carried out for the conventional solution to the elastohydrodynamic lubrication problem.

3. RESULTS AND DISCUSSION

The validation of the numerical method employed in the paper is explained in detail by Al-samieh [24]. The results showed that very good agreement for the numerical results and that published by Jalali-Vahid et al. [37] under the conditions that the elastohydrodynamic contribution dominates the generation of contact pressure.

For investigating the mechanism of fluid film formation in a very thin liquid lubricant, confined between two solid surfaces for different values of elliptical ratio, a number of simulation studies have been undertaken for the contact of Mica solid surfaces with OMCTS as the intervening fluid. The contribution to fluid film formation by viscous action can be estimated, using either Hamrock and Dowson's [15] or Brewe el al. [38] extrapolated oil film thickness equations, both for elliptical point contact geometries under iso-viscous elastic or iso-viscous rigid regime of lubrication respectively. Table 1 lists the physical properties of the system. These conditions yield lightly loaded contacts, which promote the formation of ultra-thin films in very small separations of molecularly smooth frictionless contacts.

Table 1. Physical and geometrical properties of contacting materials and OMCTS lubricant.

Viscosity η_o	2.35 mPa.s	**Pressure of viscosity coefficient α**	10 GPa^{-1}
ε	5.83x10^{-10} Pa	ξ	1.68x10^{-9} Pa
Molecular diameter, a	1 nm	**Radius of curvature of solid A in x-direction**	R_{Ax}=0.01111 (m)
Young's modulus E_A	34.5 GPa	**Radius of curvature of solid A in y-direction**	R_{Ay}=0.01111 (m)
Young's modulus E_B	34.5 GPa	**Radius of curvature of solid B in x-direction**	R_{Bx}= ∞ (m)
Poisson's ratio ν_A	0.205	**Poisson's ratio ν_B**	0.205

Details for different sets of numerical results are recorded in Table 2. As shown in table, four sets of results for different operating conditions have been collected for different elliptical ratio, to investigate the mechanism of fluid film formation in ultra-thin film conjunctions. In these sets, the dimensionless parameters G^* and U^* have been kept constant, and the applied load has been changed from (0.01-10) mN, for elliptical ratio of 2, 3, 4 and 6. The collected numerical results for minimum film thickness due to hydrodynamic action alone is shown in the twelfths column, while column thirteen shows the calculated minimum film thickness according to Hamrock and Dowson [15] or Brewe et al. [38] extrapolated oil film thickness formulae under iso-viscous elastic or iso-viscous rigid regime of lubrication respectively. Column fifteen of the same table shows the collected numerical results for minimum film thickness as the result of combined viscous action and surface forces of Van der Waals' and solvation.

The simulation studies were carried out with computational meshes with nodal densities in the range 10000-60000, according to the required inlet distance and the applied load to satisfy the convergence criteria, as well as ensuring fully flooded conditions. In fact, if the nodal density was increased, a larger number of nodes would fall into the region of the pressure spike for the case of EHL and this would result in its better resolution (i.e. the predicted magnitude becomes higher). Elsewhere the transient pressure values are almost identical. This feature had been shown by Al-samieh and Rahnejat [39]. In the figures shown below, the oscillatory nature of solvation pressure is aided to the hydrodynamic pressure in case of ultrathin film. In this case, the nodal density is chosen in such that by further increase the nodal density, the results cannot be affected.

Figure 2 shows the pressure distribution and the corresponding oil film thickness shape as the result of viscous action only in the direction of entraining motion through the central line of contact for the case of (36) of Table 2 where the ellipticity ratio equal 4. The mode of lubrication for the above-mentioned case is iso-viscous rigid in the Greenwood chart [40]. Verification of the numerical predictions has been made with the extrapolated oil film thickness formula ("equation (14)") reported by Brewe et al. [38] as follows:

$$\{H_{\min}\}_{I.R} = \hat{H}\left(\frac{U^*}{W^*}\right)^2 \tag{14}$$

where,

$$\hat{H} = 128\beta\phi^2\left[0.13\tan^{-1}\left(\frac{\beta}{2}\right)+1.68\right]^2,\ \beta = \frac{R_y}{R_x} \approx \left(\frac{K}{1.03}\right)^{1/0.64},$$

$$\phi = \left(1+\frac{2}{3\beta}\right)^{-1}$$

Table 2. Comparison between numerical results and the existing extrapolated oil film thickness formula of Hamrock and Dowson [15] or Brewe et al. [38].

Set No.	K	Case No.	w (mN)	W* X10-11	G*	u (μm/s)	U* X10-16	G_e	G_v	Regime	$h^*_{\min}$ (nm)	$\bar{h}_{\min}$ (nm)	Error % $\frac{h^*_{\min}-\bar{h}_{\min}}{\bar{h}_{\min}}$	$h_{\min s}$ (nm)
1	6	1	0.01	0.225	360	100	5.87	0.25162	0.01187	-	6.971	-	-	6.991
		2	0.02	0.449				1.59768	0.09498	-	6.149	-	-	6.659
		3	0.03	0.675				4..7106	0.32055	-	5.529	-	-	5.664
		4	0.04	0.899				10.1447	0.75983	-	5.053	-	-	5.661
		5	0.05	1.124				18.3935	1.48405	-	4.650	-	-	5.637
		6	0.06	1.349				29.9099	2.5644	-	4.332	-	-	5.637
		7	0.07	1.574				45.1171	4.07223	-	3.985	-	-	4.731
		8	0.08	1.799				64.4149	6.07867	-	3.764	-	-	4.723
		9	0.09	2.024				88.1847	8.65499	-	3.620	-	-	4.673
		10	0.1	2.248				116.819	11.8690	-	3.449	-	-	4.668
		11	0.2	4.497				742.195	95.016	-	2.287	-	-	4.650
		12	0.3	6.745				2187.81	320.606	-	1.823	-	-	3.861
		13	0.4	8.994				4708.78	759.834	-	1.752	-	-	3.840
		14	0.5	11.24				8537.60	1484.05	*I.R*	1.662	1.954	14.9	3.820
		15	0.7	15.74				20960.6	4074.18	*I.R*	0.997	0.998	0.10	3.820
		16	1	22.48				54210.5	11872.4	*I.E*	0.877	0.957	8.36	3.798
		17	1.5	33.73				159831	40069.4	*I.E*	0.775	0.879	11.83	3.759
		18	2	44.97				344216	94979.3	*I.E*	0.722	0.827	12.69	3.692
		19	4	89.94				2185642	759834	*I.E*	0.615	0.715	13.9	2.870
		20	6	134.9				6444012	2564442	*I.E*	0.571	0.657	13.10	2.855
		21	8	179.9				$1.4X10^7$	6078677	*I.E*	0.541	0.618	12.45	2.841
		22	10	224.8				$2.5X10^7$	$1.2X10^7$	*I.E*	0.537	0.590	8.98	2.830
2	4	23	0.01	0.225	360	100	5.87	0.25162	0.01187	-	5.992	-	-	6.690
		24	0.02	0.449				1.59768	0.09498	-	5.220	-	-	5.685
		25	0.03	0.675				4..7106	0.32055	-	3.819	-	-	5.665
		26	0.04	0.899				10.1447	0.75983	-	3.495	-	-	5.582
		27	0.05	1.124				18.3935	1.48405	-	3.244	-	-	4.738
		28	0.06	1.349				29.9099	2.56444	-	2.953	-	-	4.698
		29	0.07	1.574				45.1171	4.07223	-	2.776	-	-	4.688
		30	0.08	1.799				64.4149	6.07867	-	2.725	-	-	4.686
		31	0.09	2.024				88.1847	8.65498	-	2.57	-	-	4.681
		32	0.1	2.248				116.819	11.8690	-	2.415	-	-	4.669
		33	0.2	4.497				742.195	95.016	-	1.377	-	-	3.858
		34	0.3	6.745				2187.81	320.606	-	1.077	-	-	3.841
		35	0.4	8.994				4708.78	759.834	*I.R*	1.146	1.487	22.9	3.825
		36	0.5	11.24				8537.60	1484.05	*I.R*	1.037	0.952	8.93	3.813
		37	0.6	13.49				13883.1	2564.44	*I.E*	0.942	0.926	1.73	3.801
		38	0.7	15.74				20941.7	4072.24	*I.E*	0.879	0.896	1.89	3.787
		39	0.9	20.24				40932.1	8654.99	*I.E*	0.805	0.850	5.29	3.761
		40	1	22.48				54210.5	11872.4	*I.E*	0.789	0.832	5.17	3.747
		41	1.5	33.73				159831	40069.4	*I.E*	0.661	0.764	13.5	2.906
		42	2	44.97				344216	94979.3	*I.E*	0.648	0.719	9.87	2.885
		43	4	89.94				2185642	759834	*I.E*	0.565	0.623	9.31	2.855
		44	6	134.9				6444012	2564442	*I.E*	0.528	0.570	7.37	2.846
		45	8	179.9				$1.4X10^7$	6078677	*I.E*	0.498	0.537	7.26	2.828
		46	10	224.8				$2.5X10^7$	$1.2X10^7$	*I.E*	0.489	0.513	4.68.	2.813

* Key: I.E: Iso-viscous Elastic I.R: Iso-viscous Rigid

Table 2. Comparison between numerical results and the existing extrapolated oil film thickness formula of Hamrock and Dowson [15] or Brewe et al. [38].

Set No.	K	Case No.	W (mN)	W^* X10^{-11}	G^*	u (μm/s)	U^* X10^{-16}	G_e	G_v	Regime	$h^*_{\min}$ (nm)	$\bar{h}_{\min}$ (nm)	Error % $\frac{h^*_{\min}-\bar{h}_{\min}}{\bar{h}_{\min}}$	$h_{\min s}$ (nm)
3	3	47	0.01	0.225	360	100	5.87	0.25162	0.01187	-	5.667	-	-	6.679
		48	0.02	0.449				1.59768	0.09498	-	4.851	-	-	5.702
		49	0.03	0.675				4..7106	0.32055	-	3.749	-	-	5.649
		50	0.04	0.899				10.1447	0.75983	-	3.399	-	-	4.713
		51	0.05	1.124				18.3935	1.48405	-	3.126	-	-	4.665
		52	0.06	1.349				29.9099	2.56444	-	3.053	-	-	4.664
		53	0.07	1.574				45.1171	4.07223	-	2.978	-	-	4.660
		54	0.08	1.799				64.4149	6.07867	-	2.953	-	-	4.660
		55	0.09	2.024				88.1847	8.65498	-	2.889	-	-	4.659
		56	0.1	2.248				116.819	11.8690	-	2.354	-	-	4.631
		57	0.2	4.497				742.195	95.016	-	1.313	-	-	3.843
		58	0.3	6.745				2187.81	320.606	-	1.022	-	-	3.822
		59	0.4	8.994				4708.78	759.834	-	0.898	-	-	3.804
		60	0.5	11.24				8537.60	1484.05	*I.R*	0.766	0.551	39.0	3.788
		61	0.7	15.74				20941.7	4072.24	*I.E*	0.760	0.791	3.92	3.753
		62	0.9	20.24				40932.1	8654.99	*I.E*	0.717	0.749	4.27	3.699
		63	1	22.48				54210.5	11872.4	*I.E*	0.707	0.734	3.68	3.683
		64	1.5	33.73				159831	40069.4	*I.E*	0.647	0.674	4.01	2.936
		65	2	44.97				344216	94979.3	*I.E*	0.557	0.634	12.15	2.872
		66	4	89.94				2185642	759834	*I.E*	0.524	0.548	4.38	2.883
		67	6	134.9				6444012	2564442	*I.E*	0.516	0.504	2.38	2.820
		68	8	179.9				1.4X10^7	6078677	*I.E*	0.449	0.474	5.27	2.846
		69	10	224.8				2.5X10^7	1.2X10^7	*I.E*	0.349	0.452	22.79	2.779
4	2	70	0.01	0.225	360	100	5.87	0.25162	0.01187	-	5.159	-	-	5.654
		71	0.02	0.449				1.59768	0.09498	-	4.317	-	-	5.630
		72	0.03	0.675				4..7106	0.32055	-	3.741	-	-	4.842
		73	0.04	0.899				10.1447	0.75983	-	3.036	-	-	4.797
		74	0.05	1.124				18.3935	1.48405	-	2.715	-	-	4.741
		75	0.07	1.574				45.1171	4.07223	-	1.409	-	-	4.691
		76	0.08	1.799				64.4149	6.07867	-	1.336	-	-	4.642
		77	0.09	2.024				88.1847	8.65498	-	1.270	-	-	4.597
		78	0.1	2.248				116.819	11.8690	-	1.261	-	-	4.543
		79	0.2	4.497				742.1952	95.01632	*I.R*	1.115	1.455	23.36	3.829
		80	0.3	6.745				187.81	0.606	*I.E*	0.816	0.771	5.84	3.784
		81	0.4	8.994				4708.78	759.834	*I.E*	0.764	0.726	5.23	3.761
		82	0.5	11.24				8537.60	1484.05	*I.E*	0.689	0.693	0.58	3.723
		83	0.7	15.74				20941.7	4072.24	*I.E*	0.646	0.645	0.16	2.898
		84	0.9	20.24				40932.1	8654.99	*I.E*	0.619	0.612	1.14	2.884
		85	1	22.48				54210.5	11872.4	*I.E*	0.607	0.599	1.34	2.879
		86	1.5	33.73				159831	40069.4	*I.E*	0.566	0.549	3.09	2.863
		87	2	44.97				344216	94979.3	*I.E*	0.543	0.518	4.83	2.849
		88	4	89.94				2185642	759834	*I.E*	0.484	0.475	1.89	2.809
		89	6	134.9				6444012	2564442	*I.E*	0.456	0.411	10.9	2.774
		90	8	179.9				1.4X10^7	6078677	*I.E*	0.351	0.387	9.3	2.706
		91	10	224.8				2.5X10^7	1.2X10^7	*I.E*	0.337	0.369	8.67	2.781

* Key: I.E: Iso-viscous Elastic I.R: Iso-viscous Rigid

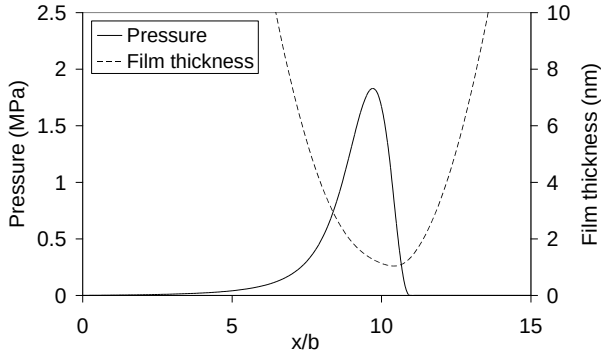

Fig. 2. Hydrodynamic pressure profile and film shape for W^* =11.24X10^{-11} and U^* =5.87X10^{-16} (F=0.5 mN, k=4, case (36)).

It can be observed from Fig. 2 that, the minimum film thickness obtained as 1.037 nm, and as 0.952 nm by using the regression formula of Brewe et al. [38] (i.e. "equation (14)") and the error is equal to 8.93 %.

Figure 3 shows the pressure distribution and the corresponding oil film thickness as the result of viscous action only in the direction of entraining motion through the central line of contact for the case (66) of Table 2 where the ellipticity ratio equal 3. The lubrication regime of the above-mentioned case pertains to the iso-viscous elastic region in the Greenwood chart [40]. In this regime of lubrication, the regression formula presented by Hamrock and Dowson [15] is used to compare the results obtained by the current numerical analysis. They generated the following dimensionless minimum oil film thickness relationship:

$$H_{\min} = 7.43(U^*)^{0.65}(W^*)^{-0.21}(1-0.85e^{-0.31K}) \quad (15)$$

It can be observed from Fig. 3 that, the minimum film thickness obtained as 0.524 nm, and as 0.548 nm by using the regression formula of of Hamrock and Dowson [15] (i.e. "equation (15)") and the error is equal to 4.38 %.

In fact, as shown from Table 2, columns twelfth, thirteen and fourteen, the results for different values of ellipticity ratio conform well to Hamrock and Dowson [15] or Brewe et al. [38] extrapolated oil film thickness formulae under iso-viscous elastic or iso-viscous rigid regime of lubrication respectively, with the error being in the range (0.1-24) %.

However, with such thin films the action of molecular forces has become significant and the mechanism of fluid film formation is no longer purely governed by the viscous action of the fluid alone. This has already been shown by Matsouka and Kato [21], Al-samieh and Rahnejat [22], Al-samieh [24], Van Megen and Snook [28], Horn and Israelachvili [29], Israelachvili et al. [30], Homola et al. [31], Israelachvili [32], Philippe Bordarier et al. [33] and Ateeque Malani and Ayappa [34].

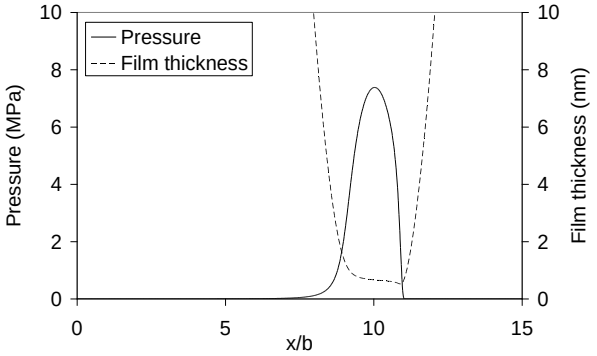

Fig. 3. Hydrodynamic pressure profile and film shape for W^* =89.94X10^{-11} and U^* =5.87X10^{-16} (F=4 mN, k=3, case (66)).

Figures 4-7 show the total pressure distribution and the corresponding elastic film shape for the central line of contact in the direction of entraining motion for cases (16), (36), (66) and (79) of table (2). The values of elliptical ratio are K = 6, 4, 3 and 2 respectively. The conditions relate to iso-viscous rigid is shown in Fig. 5 and 7 where as the conditions relate to iso-viscous elastic is shown in Figs. 4 and 6. It can be seen that from Figs. 4-7 an oscillatory pressure distribution due to solvation pressure is observed and an elastically deformed flattened solid surfaces is appeared. In fact, the load carried by the lubricant is shared by a combined mechanism of pressure generation in the contacting region as shown by equation (1). In the case of Van der Waals' force the attractive nature of the force leads to suction (i.e. negative pressures). This force, therefore, tends to bring the two surfaces together. The oscillatory (attraction-repulsion) nature of solvation can also contribute to such an effect. Negative pressures caused by Van der Waals' and oscillatory solvation pressures reduce the load carrying capacity. Therefore, the repulsive net total pressure contribution from hydrodynamic action and solvation pressures, balances the constant applied load under steady state entraining motion. This yields the gap size.

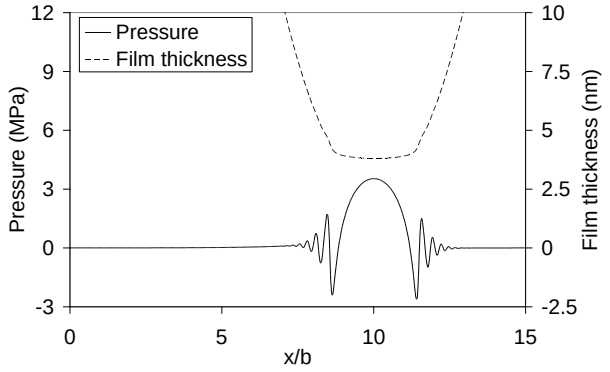

Fig. 4. Total pressure profile and film shape for W^* =22.48X10^{-11} and U^* =5.87X10^{-16} (F=1 mN, k=6, case (16)).

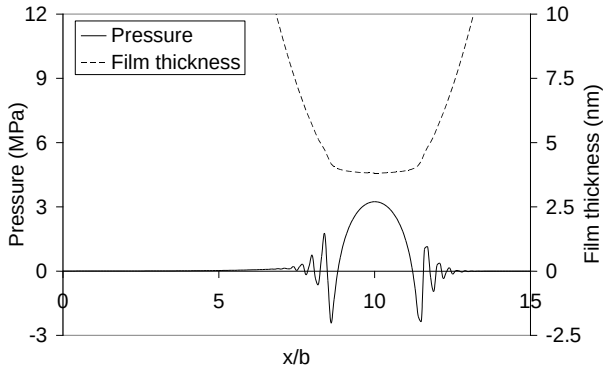

Fig. 5. Total pressure profile and film shape for W^* =11.24X10^{-11} and U^* =5.87X10^{-16} (F=0.5 mN, k=4, case (36)).

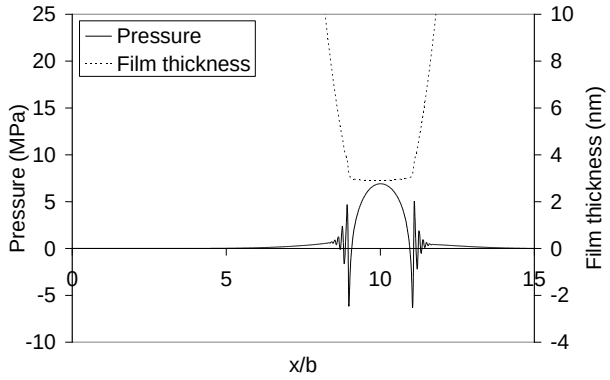

Fig. 6. Total pressure profile and film shape for W^* =89.94X10^{-11} and U^* =5.87X10^{-16} (F=4 mN, k=3, case (66)).

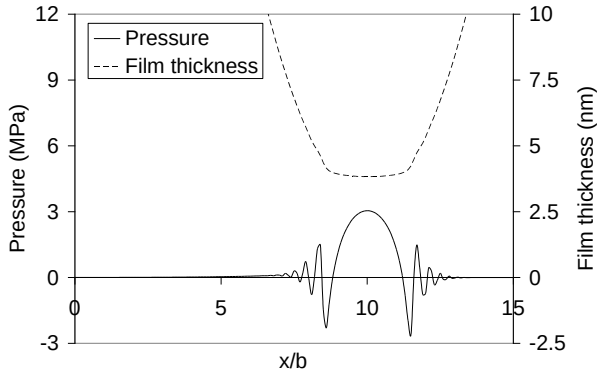

Fig. 7. Total pressure profile and film shape for W* =4.497X10^{-11} and U^* =5.87X10^{-16} (F=0.2 mN, k=2, case (79)).

As can be noticed from Table 2 the film thickness due to hydrodynamic action alone for the previous cases of (16, 36, 66 and 79) is 0.877, 1.037, 0.524 and 1.115 nm respectively and that due to the combined effect of hydrodynamic action, Van der waal's and solvation pressure is 3.798, 3.813, 2.883 and 3.829 nm respectively as shown in Figs. 4-7. In fact, the film thickness is approximately the same about 3.8 nm for the cases that shown in Figs. 4, 5 and 7 while that shown in Fig. 6 are about 2.9 nm. It is clear that, the viscous action is negligible for the case (66) that shown in Fig. 6 and the intermolecular force is dominant in determining the film thickness, the effect of hydrodynamic action accounts for less than 18 % of the actual film thickness. By comparing those figures it can be seen that the maximum pressure in Fig. 6 is approximately twice larger than that in Figs. 4, 5 and 7. Thus, the pressure due to intermolecular force of Van der waal's and solvation is larger but generated in a smaller area. This explanation has been shown by Kato and Matsouka [23], and Al-samieh and Rahnejat [22]. Generally, as shown in Table 2, the overall film thickness as a combined effect of hydrodynamic action and an intermolecular forces of Van der Waals' and solvation forces is between (7 – 2.7) nm, whereas the numerically predicted value for hydrodynamic action alone is between (7 - 0.3). In fact, the effect of hydrodynamic action is less than (18-30) % of the actual film as the film thickness is reduced below 7 nm for different values of elliptical ratio. This finding is in-line with those of Matsuoka and Kato [21] and Al-samieh and Rahnejat [22] although both of these contributions describe behaviour of ultra-thin films in circular point contact.

Figures 8-11 show the variation of lubricant film thickness with applied load for different values of elliptical ratio of K = 6, 4, 3 and 2 respectively. The speed of entraining motion is 100 μm/s. In each figure, there are three curves, one illustrating the overall minimum oil film thickness as the result of combined viscous action and surface force of Van der Waal's and solvation. The other two gives the contribution due to hydrodynamics action alone; one for the numerically predicted values and the other gives the calculated values using Hamrock and Dowson [15] extrapolated oil film thickness formula under iso-viscous elastic regime of lubrication or Brewe et al. [38] extrapolated formula for iso-viscous rigid for elliptical point contacts.

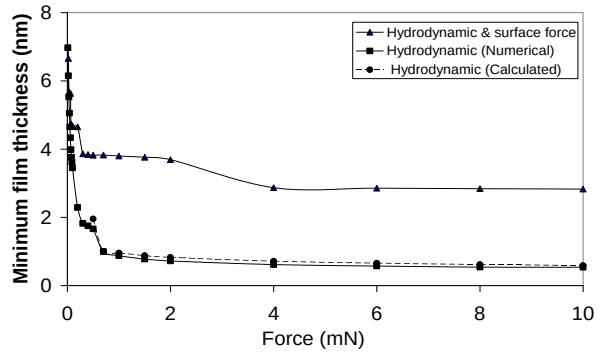

Fig. 8. Variation of film thickness with applied load for $U^*=5.87X10^{-16}$, K=6.

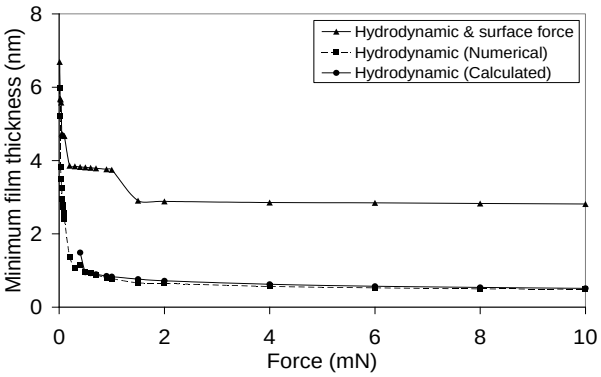

Fig. 9. Variation of film thickness with applied load for $U^*=5.87\ X10^{-16}$, K=4.

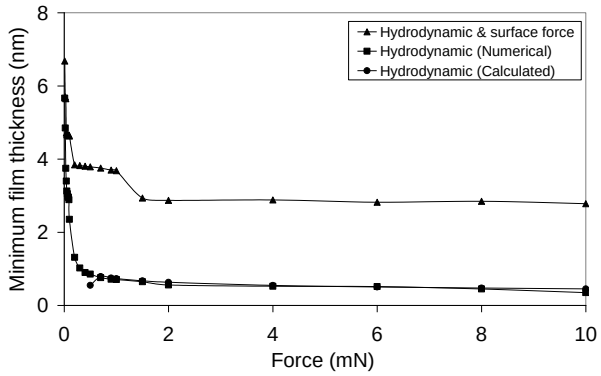

Fig. 10. Variation of film thickness with applied load for $U^*=5.87X10^{-16}$, K=3.

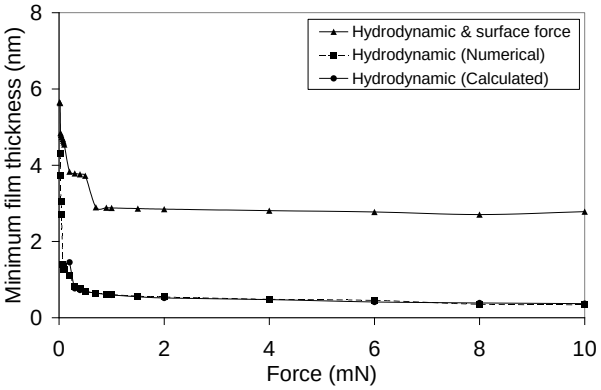

Fig. 11. Variation of film thickness with applied load for $U^*=5.87X10^{-16}$, K=2.

It can be observed from these figures that, when the hydrodynamic action is associated with the action of surface force of Van der Waal's and solvation pressure and as the film thickness is reduced below about 7 nm the overall film thickness is much larger than those predicted by either of the formulae, because they do not take into account the dominant regime of lubrication, which is due to surface forces and a discretization of the film thickness is observed in all the cases for different values of ellipticity ratio as shown in Figs. 8-11, this mean that, the film thickness remains constant even if the fluid force increases and then jumps down suddenly to the next stable thickness when the fluid force amounts to some large enough value. The interval of the discretized film thickness is about 1 nm, which corresponds roughly to the molecular diameter of OMCTS. This behaviour (discreization of the film thickness) is observed in all the cases for different values of ellipticity ratio.

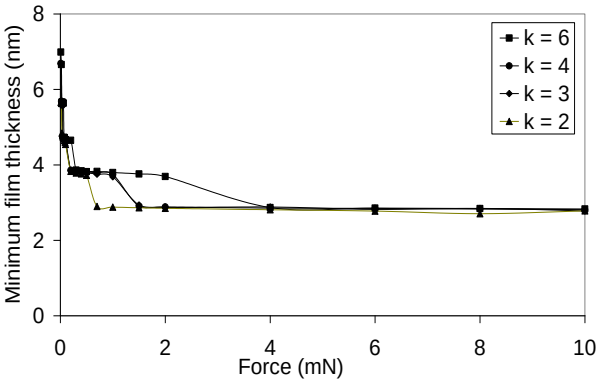

Fig. 12. Variation of film thickness with applied load for $U^*=5.87X10^{-16}$.

Finally, the variation of film thickness in the central line of contact with applied load for different set of elliptical ratio has been shown in Fig. 12 for the case where the hydrodynamic action and surface force of Van der waal's and solvation pressure is taken into account in determining the oil film thickness. It is clear that, as the applied load is increased at the constant speed of entraining motion, the film thickness is reduced and lubricant discretisation appears and the effect of intermolecular action of Van der Waal's and solvation becomes more dominant for film thickness below 7 nm for different values of ellipticity ratio (from 6 to 2) and with a constant applied load, constant speed of entraining motion and other governing parameters, the film thickness is reduced for lower values of ellipticity ratio. This is because

that, by decreasing the value of ellipticity ratio from 6 to 2, the contact area is reduced and tends to a circular point contact for ellipticity ratio of 1. This issue has been discussed in many previous publications such as that shown by Hamrock and Dowson [15] and Jalali-Vahid et al. [37]. This mean that, changing the ellipticity ratio maintain the general behavior of the formation of ultra-thin lubricating film thickness under combined actions of hydrodynamic and surface force effects as in the case of circular point contact problem (i.e. discretization of film thickness).

4. CONCLUSION

In conclusion, changing the ellipticity ratio maintain the general behaviour of the formation of ultra-thin lubricating film thickness as in the case of circular point contact problem under combined actions of hydrodynamic and surface force effects when the contiguous solids are subject to light-to-medium contact loads. The lubricant film thickness begins to deviate from the conventional lubrication theory and discretization of the film thickness is observed for all different values of ellipticity ratio and the film thickness is reduced for lower values of ellipticity ratio. The significant contribution of molecular forces in the formation of films in ultra-thin conjunctions has been demonstrated. The hydrodynamic action plays a diminishing role, and becomes almost insignificant as the intervening gap becomes one of several orders of magnitude of the molecular diameter of the intervening fluid. Although the film thickness has been predicted using extrapolated oil film formulae obtained in such regions of lubrication charts, the paper shows that the actual film thickness values far exceed these predictions. This finding conforms to the conclusions of Matsuoka and Kato [21] and Al-samieh and Rahnejat [22], although both of these contributions describe steady behaviour of ultra-thin films in circular point contact.

REFERENCES

[1] T. Becker and F. Mugele, 'Nanofluidics: Molecularly thin lubricant layers under confinement', *Molecular Simulation*, vol. 31, no. 6, pp. 489-494, 2005.

[2] R.I. Tanner and A. Jabbarzadeh, 'Thin-film lubrication nano-rheology via molecular dynamics', *Australian Journal of Mechanical Engineering*, vol. 5, no. 1, pp. 43-50, 2008.

[3] J. Manojlović, 'Dynamics of SAMs in Boundary Lubrication', *Tribology in Industry*, vol. 35, no. 3, pp. 200-207, 2013.

[4] C. Xiankun, S. Tianmin, W. Shizhu and Y. Yuan, 'Micro/Nanotribological and Mechanical Studies of TiN Thin-Film for MEMS Applications', *STLE Tribology Transaction*, vol. 47, no. 2, pp. 227-232, 2004.

[5] M. Teodorescu, S. Theodossiades and H. Rahnejat, 'Impact dynamics of rough and surface protected MEMS gear', *Tribology International*, vol. 42, no. 1, pp. 197-205, 2009.

[6] L. Xiaobai, L.H. Melany and C. Tim, 'A contact model for normal immersed collisions between a particle and a wall', *Journal of Fluid Mechanics*, vol. 691, no. 2, pp. 123-145, 2012,

[7] D.Y.C. Chan and R.G. Horn, 'The drainage of thin liquid films between solid Surface', *Journal of Chemical Physics*, vol. 83, no. 24, pp. 5311-5324, 1984.

[8] S. Jang and J. Tichy, 'Rheological models for thin film EHL contacts', *Transaction ASME, Journal of Tribology*, vol. 117, no. 1, pp. 22-28, 1995.

[9] L. Jianbin, Q. Linmao, W. Shan, W. Liu and W. Shizhu, 'The Failure of Fluid Film at Nano-Scale', *STLE Tribology Transaction*, vol. 42, no. 4, pp. 912-916, 1999.

[10] M. Hartl, I. Krupka, R. Poliscuk, M. Liska, J. Molimard, M. Querry and P. Vergne, 'Thin Film Colorimetric Interferometry', *STLE Tribology Transaction*, vol. 44, no. 2, pp. 270-276, 2001.

[11] G.E. Morales-Espejel, M.L. Dumont, P.M. Lugt and A.V. Olver, 'A Limiting Solution for the Dependence of Film Thickness on Velocity in EHL Contacts with Very Thin Films', *STLE Tribology Tra*nsaction, vol. 48, no. 3, pp. 317-327, 2005.

[12] G. Dalmaz, 'Film thickness and traction measurements in small elastohydrodynamic elliptical contacts', *Proceedings of the 5th Leeds-Lyon Symposium on Tribology*, pp. 71-80, 1987.

[13] G.J. Johnston, R. Wayte and H.A. Spikes, 'The measurement and study of very thin lubricants films in concentrated contacts', *STLE Tribology Transaction*, vol. 34, no. 2, pp. 187-194, 1991.

[14] D. Cooper and A.J. Moore, 'Application of the ultrathin elastohydrodynamic oil film thickness technique to the study of automotive engine oils', *Wear*, vol. 175, no. (1-2), pp. 93-105, 1994.

[15] B.J. Hamrock and D. Dowson, 'Elastohydrodynamic lubrication of elliptical contacts for materials of low elastic modulus, Part I- Fully flooded conjunction', *Transaction ASME, Journal of Tribology*, vol. 100, no. 2, pp. 236-245, 1978.

[16] R.P. Glovnea, A.V. Olver and H.A. Spikes, 'Experimental Investigation of the Effect of Speed and Load on Film Thickness in Elastohydrodynamic Contact', *STLE Tribology Transaction*, vol. 48, no. 3, pp. 328-335, 2005.

[17] G. Guanteng and H.A. Spikes, 'Behaviour of lubricants in the mixed elastohydrodynamic regime', *Proceedings of 21st Leeds-Lyon Symposium on Tribology, Leeds*, pp. 479-485, 1994.

[18] M. Smeeth and H.A. Spikes, 'The formation of viscous surface films by polymer solutions: Boundary or elastohydrodynamic lubrication', *STLE Annual Meeting in Chicago*, no. 95-NP-7D-2, 1995.

[19] H.K. Christensen, R.G. Horn and J.N. Israelachvili, 'Measurement of forces due to structure in hydrocarbon liquids', *Journal of Colloid and Interface Science*, vol. 88, no. 1, pp. 79-88, 1982.

[20] M.L. Gee, P.M. Mcguiggan, J.N. Israelachvili and A.M. Homola, 'Liquid to solid like transition of molecularly thin films under shear', *Journal of Chemical Physics*, vol. 93, no. 3, pp. 1895-1906, 1990.

[21] H. Matsuoka and T. Kato, 'An ultrathin liquid film lubrication theory-Calculation method of solvation pressure and its application to the EHL problem', *Transaction ASME, Journal of Tribology*, vol. 119, no. 1, pp. 217-226, 1997.

[22] M.F. Al-samieh and H. Rahnejat, 'Nano-lubricant film formation due to combined elastohydrodynamic and surface force action under isothermal conditions', *Proceedings Institution of Mechanical Engineering*, *Part C*, vol. 215, no. 9, pp. 1019-1029, 2001.

[23] T. Kato and H. Matsuoka, 'Molecular layering in thin-film elastohydrodynamics', *Proceedings of the Institution of Mechanical Engineering, Part J*, vol. 213, no. 5, pp. 363-370, 1999.

[24] M.F. Al-samieh, 'Ultra-thin lubricating film due to combined elastohydrodynamic and surface force action in elliptical contact', *Engineering and Science Research Journal*, Faculty of Engineer, Shoubra, vol. 4, no. 2, pp. 5-12, 2012.

[25] D. Dowson and G.R. Higginson, 'A numerical solution to the elastohydrodynamic problem', *Journal of Mechanical Engineering Science*, vol. 1, no. 1, pp. 6-15, 1959.

[26] C.J.A. Roelands, 'Correlation aspects of viscosity-temperature-pressure relationship of lubricating oils', *PhD thesis*, Delft University of Technology, The Netherlands, 1966.

[27] B.J. Hamrock and D. Dowson, 'Isothermal elastohydrodynamic lubrication of point contact. Part I- theoretical formulation', *Transaction ASME, Journal of Tribology*, vol. 98, no. 2, pp. 223-229, 1976.

[28] W. Van Megen and I. Snook, 'Solvent structure and solvation forces between solid bodies', *Journal of Chemical Socity, Faraday Transaction II*, vol. 75, pp. 1095-1102, 1979.

[29] G. Horn and J.N. Israelachvili, 'Direct measurement of structural forces between two surfaces in a nonpolar liquid', *Journal of Chemical Physics*, vol. 75, no. 3, pp. 1400-1411, 1981.

[30] J.N. Israelachvili, P.M. Mcguiggan and A.M. Homola, 'Dynamic properties of molecularly thin liquid films', *Science*, vol. 240, no. 4849, pp. 189-191, 1988.

[31] A.M. Homola, J.N. Israelachvili, M.L. Gee and P.M. Mcguiggan, 'Measurements of and relation between the adhesion and friction of two surfaces separated by molecularly thin liquid films', *Transaction ASME, Journal of Tribology*, vol. 111, no. 3, pp. 675-682, 1989.

[32] J.N. Israelachvili, *Intermolecular and surface forces*. New York, 2nd edition, Acdemaic Press, 1991.

[33] Philippe Bordarier, Bernard Rousseau and H. Alain Fuchs, 'Solvation Force and Confinement-Induced Phase Transitions of Model Ultra Thin Films', *Molecular Simulation*, vol. 17, no. 4-6, pp. 199-215, 1996.

[34] Ateeque Malani and K.G. Ayappa, 'Confined fluids in a Janus pore: influence of surface asymmetry on structure and solvation forces', *Molecular Simulation*, vol. 38, no. 13, pp. 1114-1123, 2012.

[35] L.S. Ornstein and F. Zernike, 'Accidental deviations of density and opalescence at the critical point of a single substance', *Proceeding of Royal Academy, Amsterdam*, vol. 17, no. 2, pp. 793-806, 1914.

[36] E.M. Lifshitz, 'The theory of molecular attractive forces between solids', *Soviet Physics, JETP*, vol. 2, no. 1, pp. 73-83, 1956.

[37] D. Jalali-Vahid, H. Rahnejat and Z.M. Jin, 'Elastohydrodynamic solution for concentrated elliptical point contact of machine elements under combined entraining and squeeze film motion', *Proceedings of the Institution of Mechanical Engineering, Part J*, vol. 212, no. 6, pp. 401-411, 1998.

[38] D.E. Brewe, B.J. Hamrock and C.M. Taylor, 'Effect of geometry on hydrodynamic film thickness', *Transaction ASME, Journal of Tribology*, vol. 101, no. 2, pp. 231-239, 1979.

[39] M.F. Al-samieh and H. Rahnejat, 'Physics of lubricated impact of a sphere on a plate in a narrow continuum to gaps of molecular dimensions', *Journal of Physics, D: Applied. Phys*ics, vol. 35, no. 18, pp. 2311-2326, 2002.

[40] J.A. Greenwood, 'Presentation of elastohydrodynamic film thickness results', *Journal of Mechanical Science*, vol. 11, no. 2, pp. 128-132, 1969.

Nomenclature

a : Lubricant molecular diameter
A : Hamaker constant
b : Radius of Hertzian contact region
C : Constant defined in equation (11)
D : Deformation influence coefficient matrix
$E_{A,B}$: Young's modulus of elasticity
E' : Reduced modulus of elasticity
G^* : Materials' parameter, $G^*=E'\alpha$
h : Lubricant film thickness
H : Dimensionless film thickness, $H=hR/b^2$
H_0 : Dimensionless central oil film thickness
l : Dimensionless side leakage boundary distance
m : Dimensionless inlet distance
n_x,n_y : Number of computational grid nodes
P : Total contact pressure
p_h : Hydrodynamic pressure
p_s : Solvation pressure due to surfaces' interaction force
p_{vdw} : Pressure due to molecular Van der Waals' force
P : Dimensionless total contact pressure, $P=p/P_{Her}$
P_h : Dimensionless hydrodynamic pressure, $P_h=p_h/P_{Her}$
P_{Her} : Maximum Hertzian contact pressure
P_s : Dimensionless solvation pressure, $P_s=p_s/P_{Her}$
P_{vdw} : Dimensionless Van der Waals' pressure, $P_{vdw}=p_{vdw}/P_{Her}$
N : Total number of mesh points
K : Elliptical ratio
R : Reduced radius of counterformal contact
w : Normal applied contact load
W^* : Load parameter, $W^*=w/E'R^2$
X,Y : Dimensionless co-ordinates, $X=x/b$, $Y=y/b$
U^* : Speed (Rolling Viscosity) parameter, $U^*=u\eta_0/E'R^2$
u : Speed of entraining motion, $u=(u_A+u_B)/2$
Z : Viscosity-pressure index
α : Pressure of viscosity coefficient
δ : Total elastic deformation
ε,ξ : Constants used in equation (4)
η : Lubricant dynamic viscosity
η_0 : Atmospheric lubricant dynamic viscosity
ν : Poisson's ratio
Ω : Under-relaxation factor
ρ : Lubricant density
ρ_0 : Atmospheric lubricant density
$\overline{\rho}$: Dimensionless lubricant density, $\overline{\rho}=\rho/\rho_0$
$\overline{\eta}$: Dimensionless lubricant viscosity, $\overline{\eta}=\eta/\eta_0$

Superscripts:
i,j : Contravariant influence coefficient indices
n : Iteration index

Subscripts:
A,B : Denote the contiguous bodies in contact
k,l : Covariant influence coefficient indices